

Chapter 15

Evolution of sedimentary environments in the subduction zone of southwest Japan: recent results from the NanTroSEIZE Kumano transect

MICHAEL B. UNDERWOOD* and GREGORY F. MOORE†

*Department of Geological Sciences, University of Missouri-Columbia, Columbia, USA

†Department of Geology & Geophysics, University of Hawaii-Manoa, Honolulu, USA

ABSTRACT

The Nankai Trough is located off the coast of southwest Japan, where the Philippine Sea plate is subducting beneath the Eurasian plate. The margin's Kii Peninsula or Kumano Basin corridor is the focal area for the Nankai Trough Seismogenic Zone Experiment (NanTroSEIZE). This multi-disciplinary, multi-stage, multi-expedition project was designed to improve our understanding of seismogenic processes along the plate interface. Drilling Stage 1 of NanTroSEIZE included Expeditions 314, 315, and 316 of the Integrated Ocean Drilling Program. Coring and logging during those three expeditions generated a wealth of new information about the stratigraphic and structural evolution of the margin. Our summary descriptions are organized into three broad domains: the Kumano (forearc) Basin; the megasplay fault zone, which is a significant out-of-sequence thrust within the accretionary prism; and the frontal thrust zone of the accretionary prism. For the most part, drilling results validate structural interpretations of 3D seismic-reflection data, but they also place invaluable constraints on the timing of such events as the initiation of forearc-basin sedimentation and the history of slip on the megasplay fault. We see many types of interaction between tectonics and sedimentation. The frontal thrust zone is dominated by packets of sand and gravel that probably accumulated within trench-floor axial channel systems prior to their accretion in the early Pleistocene. The accretionary prism becomes progressively older toward land, and a time-transgressive unconformity separates the prism from the overlying slope apron. Turbidite sedimentation within the Kumano Basin did not begin until the early Pleistocene, after a succession of precursor events: formation of the underlying accretionary prism during the late Miocene and early Pliocene; erosion of an unconformity above the accretionary prism, with an associated hiatus of ~ 1.2 Myr; a long phase of unusually slow hemipelagic sedimentation, lasting from ~ 3.8 Myr to ~ 1.67 Myr; acceleration of uplift along the megasplay fault at ~ 1.55 Myr, which enhanced accommodation space; and organization of a robust sediment-delivery system, which was achieved through uplift and erosion of the hinterland and incision of canyons and gullies into the upper trench slope.

Keywords: Integrated Ocean Drilling Program; Nankai Trough; forearc basin; accretionary prism; lithostratigraphy

INTRODUCTION

The Nankai Trough subduction zone is, arguably, the world's most thoroughly studied sedimentary system of its type (Fig. 15.1). The plate boundary is

a tectonic product of Philippine Sea plate subduction beneath southwest Japan, and one of its more unusual attributes is the absence of an associated chain of active (Quaternary) volcanoes. Plate convergence occurs at a rate of ~ 4.0 – 6.5 cm/yr and at

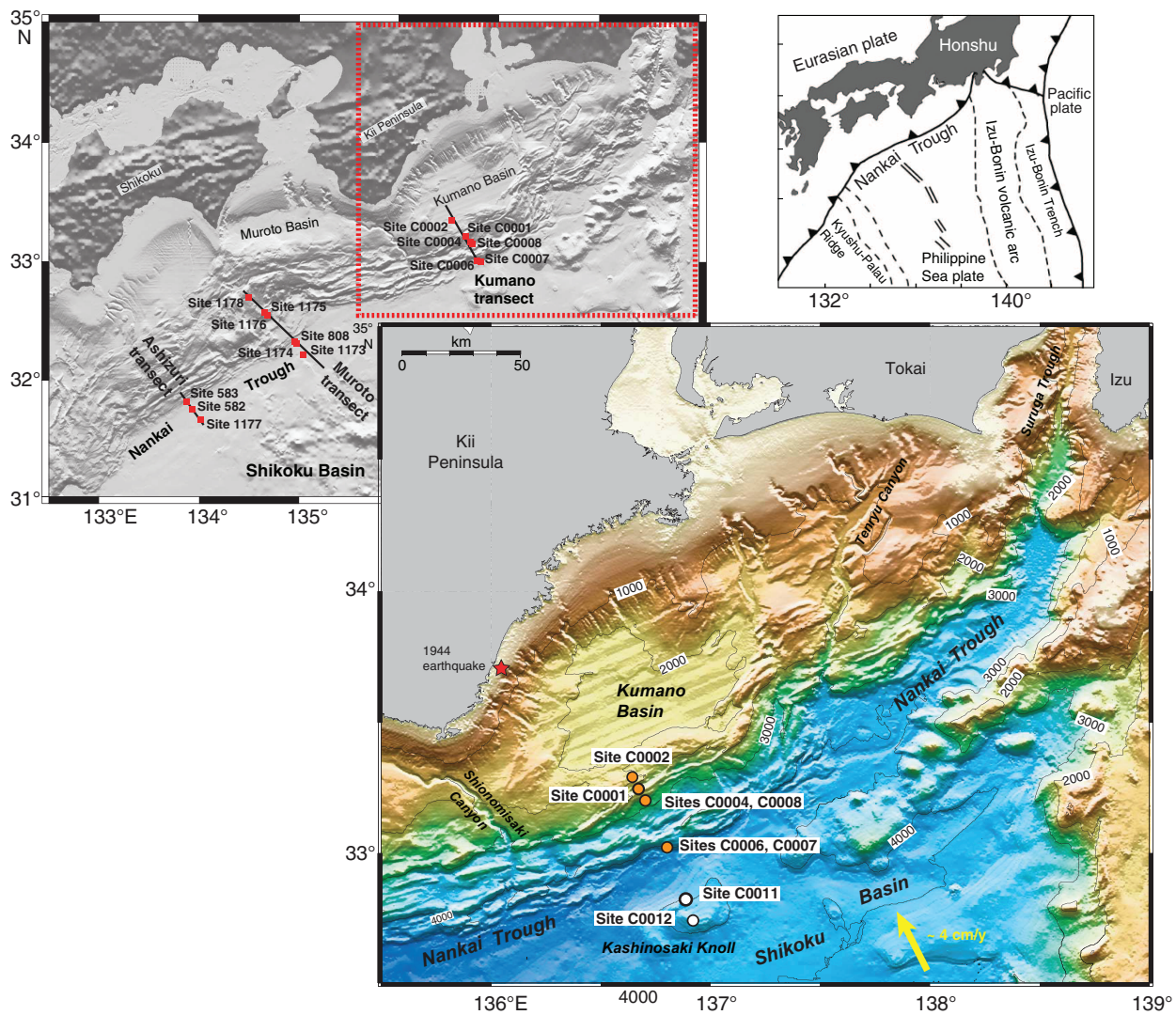


Fig. 15.1. Index map showing the Kumano transect area for the Nankai Trough Seismogenic Zone Experiment (offshore Kii Peninsula), as well as the Muroto and Ashizuri transects drilled previously by the Deep Sea Drilling Project and the Ocean Drilling Program. After Moore et al. (2009).

an azimuth of $\sim 300\text{--}315^\circ$ (Seno et al., 1993; Miyazaki and Heki, 2001; Zang et al., 2002). The Nankai system represents one end of the accretion-erosion continuum, characterized by thick accumulations of sediment (>1000 m) outboard of the deformation front and high rates of subduction accretion at the prism toe (Underwood and Moore, 1995; Clift and Vannucchi, 2004). Broadly similar conditions exist in the Cascadia Basin (Kulm and Fowler, 1974; Carlson and Nelson, 1987; MacKay et al., 1992; Underwood et al., 2005), the Aleutian Trench (Piper et al., 1973; Scholl, 1974; McCarthy and Scholl, 1985; Lewis et al., 1988; Gutscher et al., 1998), the Sunda Trench (Karig et al., 1978;

Moore et al., 1980; Beaudry and Moore, 1985; Kopp et al., 2001; Kopp and Kukowski, 2003; Fisher et al., 2007), and southern Chile (Schweller et al., 1981; Thornburg and Kulm, 1987).

Nankai has been the focus of scientific ocean drilling over four decades by the Deep Sea Drilling Project (DSDP Legs 31 and 87) (Karig et al., 1975; Coulbourn, 1986; Kagami et al., 1986), the Ocean Drilling Program (ODP Legs 131, 190 and 196) (Taira et al., 1991; Pickering et al., 1993; Moore et al., 2001; Mikada et al., 2005), and the Integrated Ocean Drilling Program (IODP Expeditions 314, 315, and 316) (Tobin et al., 2009a). In addition to the three drilling transects shown on Figure 15.1

(designated Ashizuri, Muroto, and Kumano), Nankai scientists have acquired an extensive catalog of 2D and 3D seismic-reflection images of the accretionary prism and subducting sediments in the Shikoku Basin (Aoki et al., 1982; Moore et al., 1990; Park et al., 2002; Bangs et al., 2004, 2006; Gulick et al., 2004; Moore et al., 2007; Ike et al., 2008a). This superb combination of geophysical data, and the ability to confirm depositional ages and lithologies from the cores, provides an unprecedented view of the margin's stratigraphic and structural evolution.

The Shikoku Basin, which is located seaward of the trench (Fig. 15.1), started to form during the late Oligocene by rifting and back-arc spreading behind the Izu-Bonin arc system (Okino et al., 1994; Kobayashi et al., 1995; Sdrolias et al., 2004). Late-stage reorientation of the spreading center and off-axis seamount volcanism continued into the middle and late Miocene, and this magmatism created significant variations in the configuration of igneous basement, including the Kinan seamount chain (Okino et al., 1994). Kashinosaki Knoll represents one such basement feature in the Kumano transect area (Ike et al., 2008a). Relief on the young basement, in turn, influenced the thickness of total sediment, which is highly variable, and the facies character of each sedimentary unit within the Shikoku Basin (Ike et al., 2008b).

The typical sedimentary responses to basement topography were for thicker intervals of Miocene turbidites to fill areas where the basement is lower, and for the basement highs to be overlain by a highly condensed section of Miocene hemipelagic mud (Underwood, 2007; Ike et al., 2008b).

As the subducting abyssal basin gradually filled with sediment, relief across the seafloor became less pronounced. Consequently, the Pliocene-Pleistocene stratigraphic intervals of the Shikoku Basin evolved to a more uniform thickness and consistent lithology, composed of hemipelagic mud with abundant interbeds of air-fall volcanic ash (Taira et al., 1991; Moore et al., 2001). Clay minerals in the Shikoku Basin also show gradual shifts through time, beginning with a Miocene, arc-derived smectite-rich assemblage and changing to younger chlorite- and illite-rich assemblages eroded from the uplifted accretionary complexes (mostly sedimentary and metasedimentary rocks) that are now exposed across the Outer Zone of Japan (Steurer and Underwood, 2003; Underwood and Steurer, 2003; Underwood and Fergusson, 2005). As subduction carries strata closer to the subduction front, the Shikoku Basin facies eventually experience rapid inundation beneath a landward-thickening wedge of trench turbidites (Fig. 15.2), which builds up the total sediment thickness by an additional 0.5 to 1.3 km

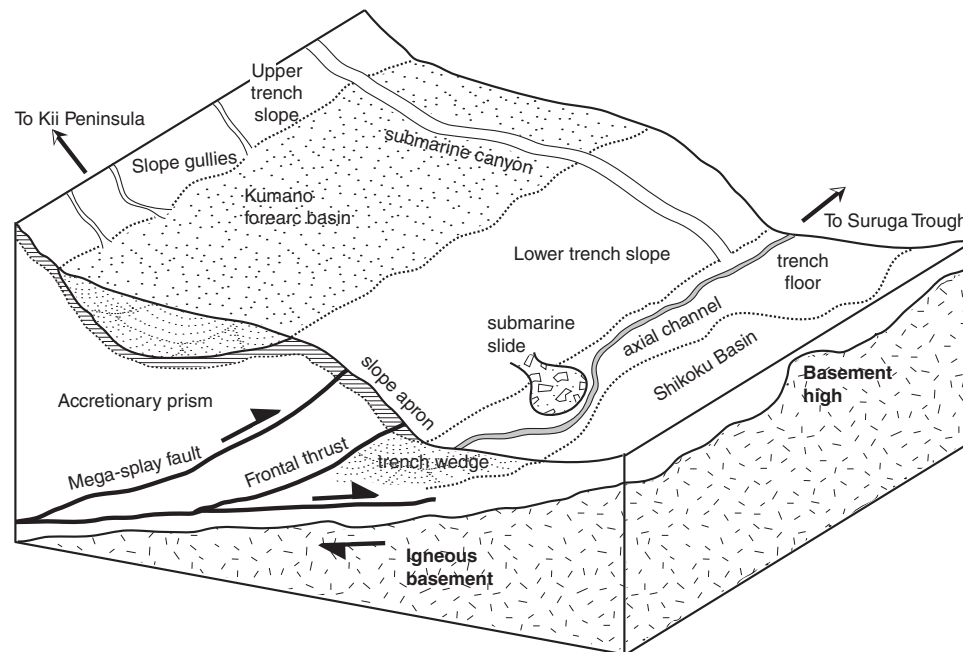


Fig. 15.2. Schematic illustration of depositional environments within the Nankai Trough subduction zone.

(Taira and Ashi, 1993; Mountney and Westbrook, 1996).

At its northeastern end, the Nankai Trough merges almost imperceptibly into the Suruga Trough, an immense submarine canyon system that was incised along the west side of the collision zone between the Izu-Bonin volcanic arc and Honshu (Fig. 15.1). Detrital provenance studies show that the primary source for the Quaternary trench wedge is this zone of rapid uplift and collision (Marsaglia et al., 1992; Underwood and Ferguson, 2005). Turbidity currents have funneled terrigenous sediment from several fluvial sources on Honshu through a series of large submarine canyons (Suruga Trough, Tenryu Canyon, Shionomizaki Canyon). These deeply incised conduits head very close to the present shoreline and thus remain active even during highstands of sea level (Soh and Tokuyama, 2002; Kawamura et al., 2009). Collectively, this combination of a coarse-grained trench-wedge turbidite facies resting above heterogeneous Shikoku Basin deposits comprises the sedimentary inputs to the subduction system (Fig. 15.2). Three-dimensional variations in those inputs help mold the structural architecture, mechanical properties, and hydrogeology of the accretionary prism (Underwood, 2007). Structural evolution of the accretionary prism, in turn, has controlled the development of sedimentary depocenters on the overriding plate, including a series of prominent forearc basins (Fig. 15.2).

The Nankai Trough Seismogenic Zone Experiment (NanTroSEIZE) is an ambitious, multi-stage, multidisciplinary project designed to improve our understanding of seismogenic processes along the

plate interface of an active subduction zone (Tobin and Kinoshita, 2006). The transect area for NanTroSEIZE is located seaward of the Kii Peninsula, Honshu, Japan (Fig. 15.1), within the confines of a recent 3D seismic reflection survey (Fig. 15.3). This study area contains several prominent features, including a large forearc basin (Kumano Basin) and a potentially seismogenic megasplay fault seaward of the forearc basin. Stage 1 of NanTroSEIZE was completed during 2007–2008. Three IODP expeditions drilled holes for coring and logging-while-drilling (LWD) measurements at eight sites; the drilling operations extended to relatively modest depths of 329 to 1401 meters below seafloor (Fig. 15.3). During Stage 2 of NanTroSEIZE, the project documented subduction inputs at two reference sites seaward of the trench (Expedition 322; Underwood et al., 2009). The ultimate scientific and technological challenges, however, will be to utilize ultra-deep riser drilling to penetrate the seismogenic plate interface at a depth of 6 to 7 km below seafloor and then install long-term borehole observatories within the fault zone (Tobin and Kinoshita, 2006).

As the opening act of Stage 1 drilling, IODP Expedition 314 focused on acquisition of logging-while-drilling data across most of the forearc and accretionary prism (Tobin et al., 2009b). Two of those six sites were then cored during Expedition 315, one above the megasplay fault zone (Site C0001) and the other (Site C0002) within the distal or seaward side of Kumano Basin (Ashi et al., 2009). After that, Expedition 316 targeted two sites across the frontal thrust zone of the accretionary prism (Sites C0006 and C0007)

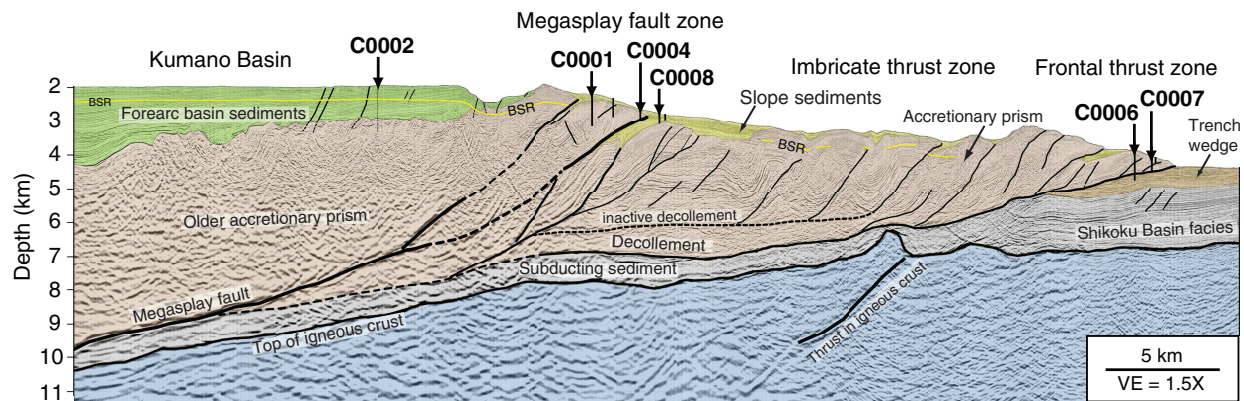


Fig. 15.3. Composite seismic line extracted from 3D seismic volume, with basic geologic interpretation. The line crosses through (or near) all NanTroSEIZE Stage 1 drill sites (Fig. 15.1). After Moore et al. (2009).

and two (Sites C0004 and C0008) above and across the shallow extension of the megasplay fault (Screaton et al., 2009a, 2009b). Data from these three expeditions finally allow the team of scientists to pin down many aspects of the margin's sedimentary and structural evolution that had been unconstrained by geophysics alone. The purposes of this chapter are twofold: to highlight some of those key shipboard discoveries and to merge the most up-to-date interpretations of the 3D seismic stratigraphy with the ground truth provided by coring.

TOE OF ACCRETIONARY PRISM

IODP Sites C0006 and C0007 are located on the first ridge landward of the frontal thrust (Fig. 15.4). The incoming sedimentary section seaward of the deformation front is ~2.4 km thick and is typical of the Nankai system, overall, with igneous basement overlain successively by Shikoku Basin strata and the Quaternary trench wedge (Fig. 15.3). From seismic data, we can see that the upper part of the trench wedge contains numerous nested channel-levée complexes, and a prominent axial channel meanders down the axial seafloor gradient from the source areas feeding into the Suruga Trough (Shimamura, 1989). Near the base of slope, a well-developed proto-thrust zone affects the upper Shikoku Basin strata and the lower trench-wedge deposits (Fig. 15.3).

The frontal thrust within the Kumano transect area is anomalous if compared to the frontal Nankai prism elsewhere (e.g., Muroto or Ashizuri). Along most parts of the Nankai margin, the dip of the frontal fault is steep (25–35°), and it extends landward only 1–2 km before merging down-dip into the basal décollement of the accretionary wedge; this typical “ramp-on-ramp” geometry places trench-wedge deposits over trench-wedge deposits (e.g., Moore et al., 1990, 2001). In contrast, the frontal fault near Sites C0006 and C0007 is a gently dipping (~7 to 8°) detachment that extends ~6 km landward and elevates both upper Shikoku Basin facies and trench-wedge facies in the hanging wall over younger trench sediments in the footwall (Fig. 15.4). At its seaward edge, the frontal fault is essentially parallel to bedding in both the hanging wall and the footwall (“flat-on-flat” geometry). The frontal thrust zone of Kumano is also dominated by steep landward-dipping subsidiary faults and local backthrusts. In

addition, a small wedge-shaped slope basin is evident landward of Site C0006 (Fig. 15.4); sediments within the basin were remobilized off the adjacent landward slope and lap onto the underlying accretionary prism. Less than 5 km landward of the frontal thrust, another prominent fault translates its hanging wall at least 1.25 km over the slope-basin fill; that thrust cuts off the top of an underlying anticline, making it an out-of-sequence thrust. The overriding block of the out-of-sequence thrust exhibits very low seismic amplitudes with little continuity, as compared to the footwall block (Fig. 15.4). Collectively, this extraordinary structural architecture of the frontal zone can be attributed to ridge or seamount subduction just west of the 3D seismic survey box; in that nearby region, the base-of-slope is scarred by a large submarine slide, which was probably mobilized by subduction of a basement high (Moore et al., 2009).

Coring at Sites C0006 and C0007 showed that the uppermost stratigraphic unit is an upward fining succession of hemipelagic mud with thin interbeds of silt, sandy silt, and fine sand turbidites, plus rare volcanic ash beds that probably entered the base-of-slope environment as air-fall tephra (Expedition 316 Scientists, 2009b, 2009c). The turbidites typically display sharp bases, plane-parallel laminae, and normal grading (Fig. 15.5). The sand component is mainly fine- to very-fine grained and consists of quartz, feldspar, lithic grains, and vitric fragments. The maximum age of these deposits is late Pleistocene (0.436 Myr, based on nannofossil events), and the inferred depositional environment is a gradual transition from uplifting accretionary prism into the slope apron.

Beneath this carapace of slope sediments lies ~422 m to ~328 m of accreted trench turbidites, with several sand-rich and gravel-rich packets (Fig. 15.4). The sand is dark gray to black and consists of metamorphic and volcanic lithic fragments with secondary quartz and feldspar. Individual sand beds reach thicknesses of 1 to 7 m thick and are internally structureless. Thinner beds typically display normal grading (Fig. 15.5). The gravel is clast-supported with no obvious matrix and is moderately sorted. Clasts are subrounded to subangular (Fig. 15.5). The clast assemblage is polymictic with grain types including chert, sandstone, mudstone, mylonitic quartzite, quartz-rich metamorphic rocks, volcanic fragments, and quartzo-feldspathic plutonic lithic fragments.

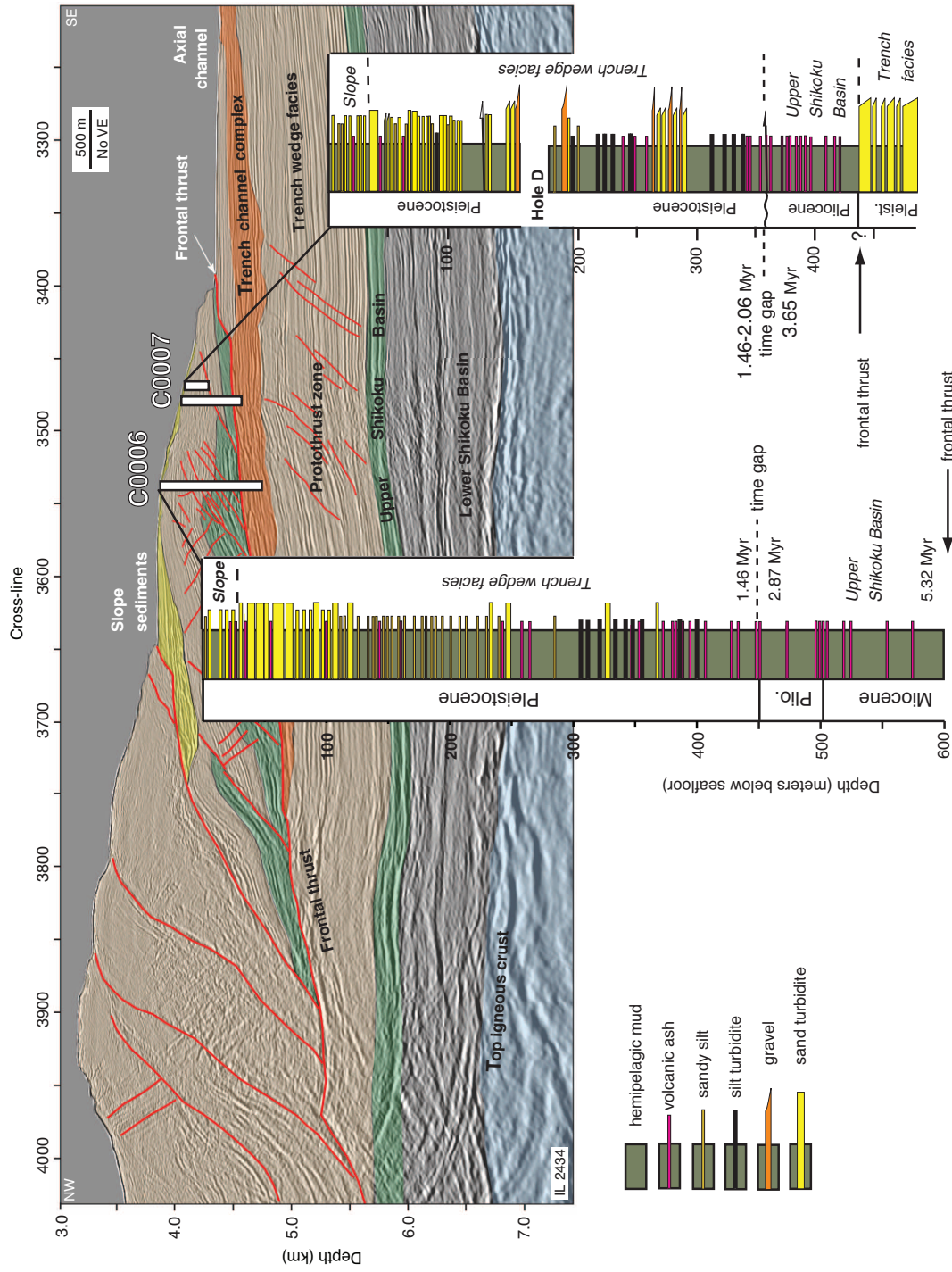


Fig. 15.4. Regional seismic line crossing IODP Sites C0006 and C0007, frontal thrust zone of the Nankai accretionary prism. Seismic interpretation is from Moore et al. (2009). Also shown are stratigraphic summaries based on the results of coring and logging-while-drilling during IODP Expeditions 314 and 316. Ages (Myr) are based on nanofossils zones.

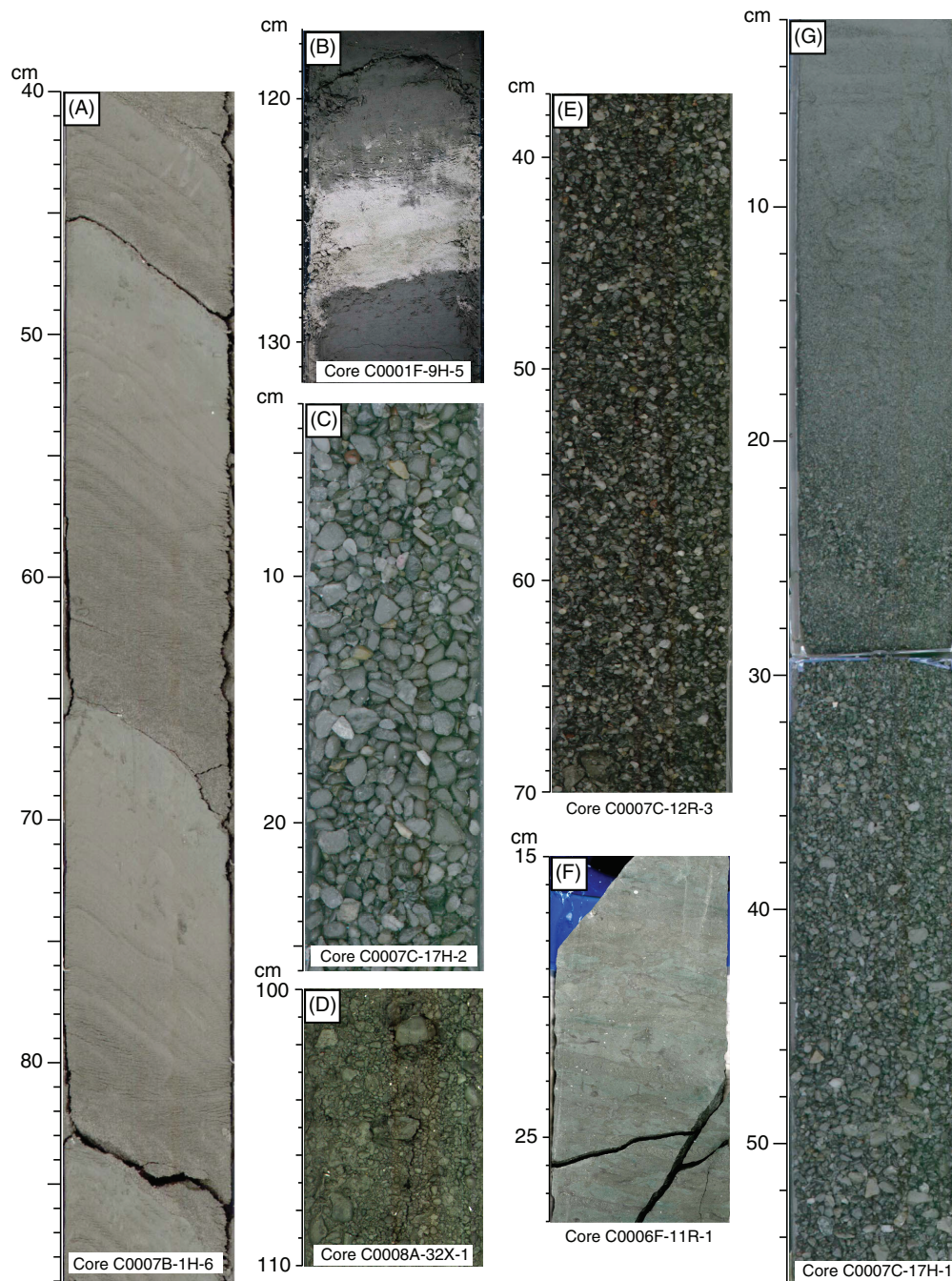


Fig. 15.5. Core photos showing representative examples of major lithologies in the Nankai Trough subduction zone. (A) Thin, fine-grained turbidites within the slope apron facies. (B) Air-fall volcanic ash deposit within the slope apron facies. (C) Polymictic gravel within the accreted trench-wedge turbidite facies. (D) Mudstone-clast conglomerate from a mass transport complex within the slope apron. (E) Coarse sand to granules within the accreted trench-wedge turbidite facies. (F) Heavily bioturbated mudstone with *Zoophycos* ichnofauna, typical of hemipelagic interbeds within most lithostratigraphic units. (G) Graded bed of granules to fine sand and silt within the accreted trench-wedge turbidite facies.

Mud-rich intervals between the sand and gravel packets are thought to represent interchannel and/or distal trench-wedge deposits. Overall, the trench-wedge facies displays a trend of thickening

and coarsening upward, with a maximum age of early Pleistocene (1.24–1.46 Myr). One way to explain this trend is as a response to the depositional site's increasing proximity to the trench axis

through time. Repetition of the sand-rich and gravel-rich packets could be a consequence of thrust faulting within the frontal prism and/or periodic migration/reactivation of the trench's axial channel prior to accretion. Although climate must have played a subsidiary role in these cycles, the age constraints from microfossils and paleomagnetism are not precise enough to correlate with global cycles of allocyclic forcing.

One of the more significant drilling discoveries during Expedition 316 is the existence of a time gap across the base of the accreted trench-wedge facies, as shown by abrupt shifts in age from 1.46 Myr to 2.87 Myr (at Site C0006) and 1.46 or 2.06 Myr to 3.65 Myr (at Site C0007). Strata below the unit boundary consist of upper Shikoku Basin facies, as exemplified by the preponderance of bioturbated hemipelagic mudstone with interbeds of volcanic ash. The maximum age of those mud/ash deposits is late Miocene (5.32 Myr). Removal of the top of the upper Shikoku Basin facies at both coring sites is enigmatic, since the contact appears to be conformable on seismic profiles (Fig. 15.4). We suggest that the missing section was removed by submarine slides on the steeply inclined flank of a subducting seamount, prior to burial beneath the trench wedge. Seismic profiles show analogous slide scars on the flanks of Kashinosaki Knoll (Fig. 15.1), which is located seaward of the trench within the Kumano transect area (Ike et al., 2008b). Deeper in the boreholes, the frontal thrust truncates the upper Shikoku Basin deposits at ~603 mbsf (Site C0006) and ~439 mbsf (Site C0007). LWD logs show clear evidence of abundant sand deposits below the frontal thrust (Expedition 314 Scientists, 2009b), but the recovery of unconsolidated sand in the footwall was minimal. The high proportion of sand beds is consistent with the seismic interpretations of the frontal thrust, which places upper Shikoku Basin facies in the hanging wall over a trench-floor axial-channel complex in the footwall (Fig. 15.4).

SEAWARD EDGE OF SPLAY FAULT SYSTEM

IODP Sites C0001, C0004, and C0008 are located on the slope of the accretionary prism, just to the southeast of a major ridge that forms the seaward boundary of Kumano Basin (Fig. 15.3). These three sites also span across the seaward edge of the megasplay fault system (Fig. 15.6). The megasplay

is regionally extensive, out-of-sequence fault system that cuts across the older part of the accretionary prism (Park et al., 2002). Appearing as a complex series of anastomosing segments, the megasplay can be traced from the seafloor to a depth of ~10 km, where the system branches off the top of the plate interface between the basal accretionary prism and subducting igneous basement (Fig. 15.3). A series of smaller thrusts within the accretionary prism offset bands of high-amplitude, laterally continuous reflections, which likely represent accreted trench-wedge and Shikoku Basin strata. Strata above some of the individual thrusts are folded into hanging wall anticlines, and the oblique dip angle of the faults creates a series of oblique ramps, the tops of which are truncated by the megasplay (Moore et al., 2007). The hanging wall above the shallow megasplay is much different than what we see in the frontal prism, characterized by low seismic amplitudes and a lack of laterally continuous seismic reflections (Fig. 15.6). That seismic character is consistent with a deformed, mudstone-dominated succession rather than extensive turbidites. Close to the seafloor, this fault block of accreted strata has moved up and over the top of younger slope-basin and slope-apron sediments, which can be traced beneath and landward of the megasplay for at least 1250 m (horizontal direction) and 750 m (vertical direction). Slope sediments also rest above the hanging-wall block, where they have been affected by slumping in several localities. As chronicled by Strasser et al. (2009), slip on the megasplay began by out-of-sequence thrusting near the prism toe at ~1.95 Myr, and after a period of relative quiescence the fault was reactivated as a major splay fault at ~1.55 Myr.

Coring revealed that the slope apron above the megasplay fault is composed of carbonate-rich, bioturbated hemipelagic mud with thin interbeds of volcanic ash (Fig. 15.6). Thin beds and irregular patches of silt, sandy silt, and fine sand are more common at Sites C0004 and C0008 than at Site C0001. At Site C0001, the lowermost 10 m of the slope apron consists of siliciclastic sand, whose grains consist mostly of detrital quartz and feldspar with abundant sedimentary and low-grade metasedimentary rock fragments (shale, argillite, chert, and quartz-mica grains). The maximum depositional age of the slope apron ranges from early Pleistocene (1.60 Myr) to late Pliocene (2.06 Myr), and its thickness ranges from 78 m (Site C0004) to 207 m (Site C0001). Mud in the slope apron contains

substantial amounts of calcareous nannofossils (up to ~25 wt-% calcite), with concentrations increasing up stratigraphic section. This trend is consistent with gradual uplift of the depositional sites above the calcite compensation depth (CCD), as seen elsewhere in the Nankai subduction system (Underwood et al., 2003).

The slope apron's base is marked by a complicated angular unconformity (Fig. 15.6). At Site C0004, the corresponding hiatus extends from

1.60 Myr to 2.06 Myr (on the basis of calcareous nannofossils), whereas the time gap at Site C0001 is from 2.06 Myr to 3.79 Myr. Immediately below the unconformity at Site C0001 we find upper Pliocene to upper Miocene accretionary-prism strata, with an age range of 3.79 to 5.32 Myr. Low seismic amplitudes indicate that this portion of the hanging wall to the megasplay is lithologically monotonous; the cores verify this interpretation, consisting mostly of carbonate-poor hemipelagic

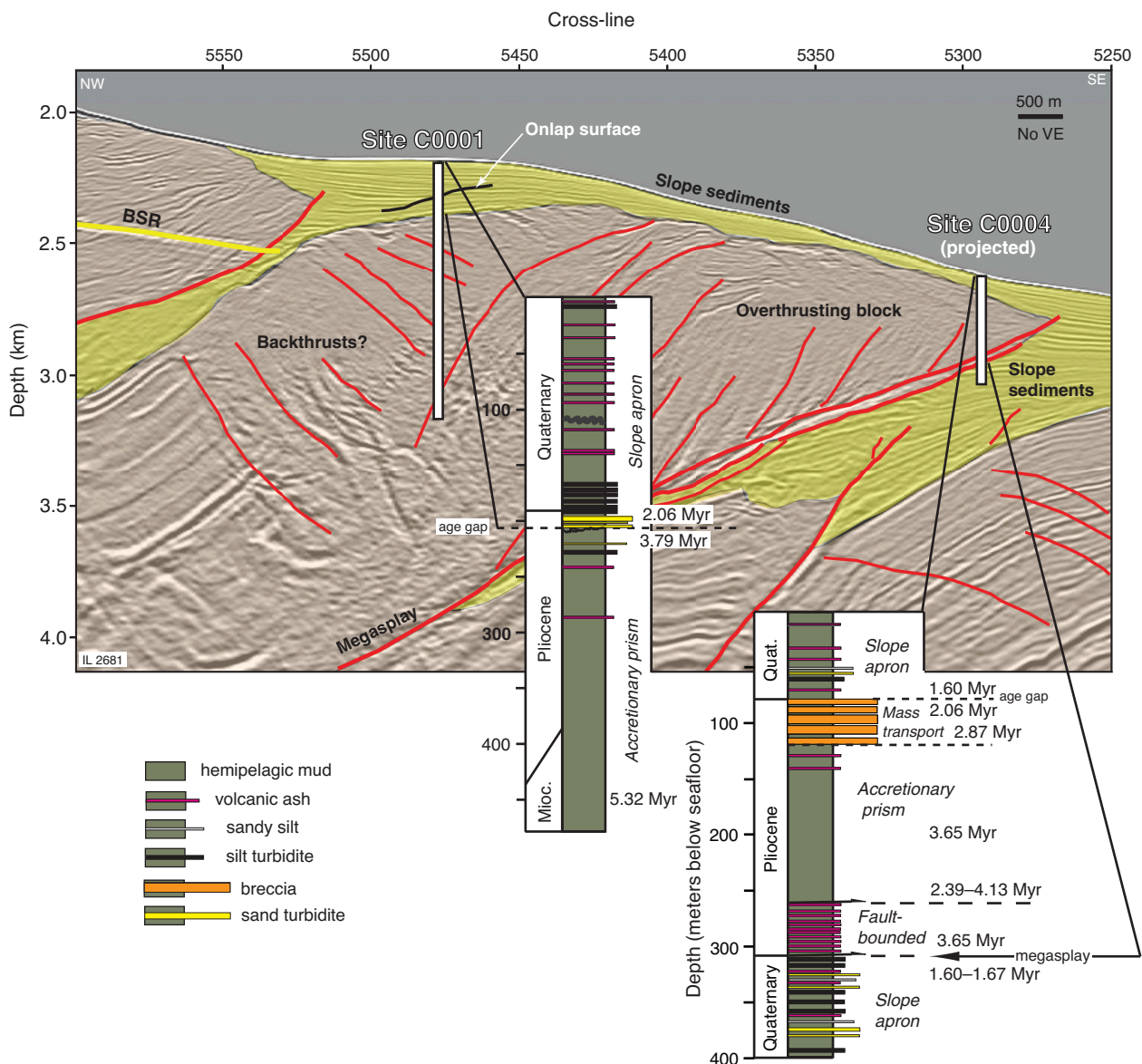


Fig. 15.6. Regional seismic line crossing IODP Sites C0001 and C0004, shallow megasplay fault zone of the Nankai accretionary prism. Seismic interpretation is from Moore et al. (2009). Also shown are stratigraphic summaries based on the results of coring and logging-while-drilling during IODP Expeditions 314, 315, and 316. Ages (Myr) are based on nannofossils zones.

mudstone (Fig. 15.6). This mudstone-rich facies stands in stark contrast to the sand- and gravel-rich units of accreted trench sediments that were cored within the frontal thrust zone (Fig. 15.4). Its original depositional environment is enigmatic but was tentatively ascribed to an unusually muddy phase of trench floor deposition below the level of the CCD (Expedition 315 Scientists, 2009a). Unfortunately, coring at this site was terminated at a depth of only 456 m below seafloor because of highly unstable hole conditions.

At Site C0004, a 40-meter-thick mass-transport complex (MTC), with clasts of hemipelagic mud, lies immediately beneath the unconformable base of the slope apron (Fig. 15.6). There is evidence for chemical alteration at the top of the mass-transport complex (e.g., pyrite). The synsedimentary breccia is matrix-supported in some places and clast-supported in others, with an age range of 2.06 to 2.87 Myr. The mud clasts could have been cannibalized either from uphill exposures of the slope apron or from the exposed top of the accretionary prism (Expedition 316 Scientists, 2009a; Strasser et al., 2009). Strata below the mass-transport complex consist of Pliocene carbonate-poor mudstone, similar to the accreted strata at C0001; the age is younger, however, equal to 2.39–4.13 Myr.

Unlike Site C0001, coring at Site C0004 actually penetrated the megasplay fault near its up-dip tip (Fig. 15.6), where roughly 50 m of Pliocene strata are sandwiched between two sub-parallel fault strands. This fault sliver contains carbonate-poor hemipelagic mudstone with unusually abundant layers of volcanic ash, and a maximum age of 3.65 Myr. Biostratigraphic correlation of the fault sliver to kindred parts of the accretionary prism remains inconclusive, but we see a substantial reversal of age across the lower of the two sub-parallel faults. Strata in the footwall are early Pleistocene in age (1.60 to 1.67 Myr); the lithologies are similar to those of the slope apron above, consisting of hemipelagic mud with moderate amounts of calcareous nannofossils. Thin graded beds of silt and silty sand turbidites are also common within this unit. Recovery of this lithologic assemblage reinforces the structural interpretation in which the hanging wall of the megasplay has overridden the slope apron (Fig. 15.6).

Site C0008 was cored seaward of the tip of the megasplay fault (Fig. 15.7). The slope apron at that locality is approximately 272 m thick and consists of two sub-units. The upper sub-unit consists of Pleistocene (maximum age of 1.67 Myr)

hemipelagic mud with moderate amounts of calcareous nannofossils and thin interbeds (<10 cm) of silt, sandy silt, and volcanic ash. Along with the normal air-fall ash layers (Fig. 15.5), this interval includes a distinctive 5-m-thick volcanoclastic sand bed with abundant basaltic rock fragments (with brown glass), pumice, and glass shards; the tephra is concentrated more near the top of the bed. Most of the terrigenous silt and sand beds are dominated by quartz, feldspar, and metasedimentary lithic fragments, but some are enriched in clear volcanic glass shards and pumice fragments. Many of the sand beds are nearly black in color due to high contents of authigenic pyrite. Overall, the proportion of sand and silt decreases up section, and the combination of lithologies is typical of the slope apron.

The underlying sub-unit is more unusual, consisting of interbedded mud-clast gravels and hemipelagic mud. The gravel beds range from 2 to 80 cm thick, and the maximum size of indurated mudstone clasts is 5 cm. Clast-matrix organization ranges from clast-supported to matrix-supported, and clast shape ranges from rounded to sub-angular (Fig. 15.5). This lower sub-unit was interpreted to be a mass-transport complex that accumulated at the base of the slope apron (Expedition 316 Scientists, 2009d). Its maximum age is 2.87 Myr (similar to the breccia deposits at Site C0004). The upper contact of the mass-transport complex is conformable, however, and its lower contact with the underlying accretionary prism also appears to be conformable judging from the geometric concordance of seismic reflections (Fig. 15.7). The accreted strata immediately below the contact are 3.65 Myr in age (ranging downward to a maximum of 5.59 Myr), so the MTC-prism boundary could be a disconformity with a modest hiatus (~0.78 Myr).

Accreted sediments below the mass-transport complex consist of fine- to coarse-grained sand and pebbly sand, with minor interbeds of hemipelagic mud. Sands are polymictic, with abundant quartz, feldspar, and heavy minerals (mostly pyroxene), plus lesser amounts of brown to black semi-opaque grains, which could be mafic to intermediate volcanic rock fragments, clay clasts, or glauconite. Pebbles include rounded fragments of basalt, plutonic rocks, schist, vein quartz, chert, sandstone, and mudstone. This lithofacies is compositionally similar to the accreted axial-channel deposits near the prism toe, so we infer a similar origin of axial turbidity currents and frontal offscraping during the early Pliocene.

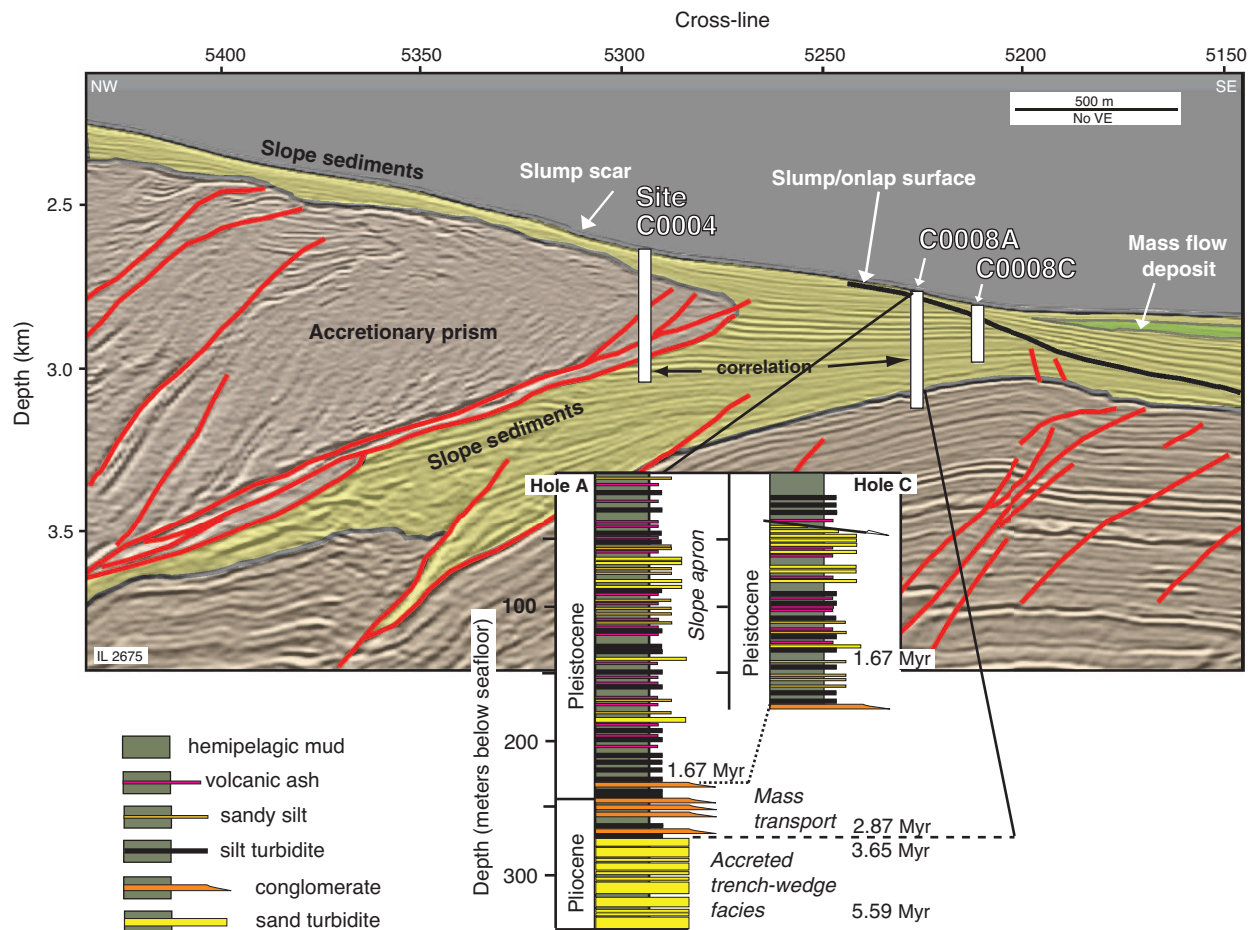


Fig. 15.7. Regional seismic line crossing IODP Sites C0004 and C0008, shallow megasplay fault zone of the Nankai accretionary prism. Seismic interpretation is from Moore et al. (2009). Also shown is the stratigraphic summary for C0008 based on the results of coring during IODP Expedition 316. Ages (Myr) are based on nanofossils zones.

KUMANO BASIN

Site C0002 is located near the seaward edge of Kumano Basin, which is one of several prominent forearc basins to dot the landscape of Nankai's upper margin (Fig. 15.1). A seismic inline through the drill site (Fig. 15.8) shows ~1000 m of relatively undeformed strata resting above an acoustic unit that displays steeply dipping, discontinuous seismic reflections (Moore et al., 2009). This style of deformation (e.g., hanging-wall anticlines, landward-dipping reflectors) is consistent with what has been imaged in other parts of the Nankai accretionary prism, including the current zone of frontal accretion. Coring into the accretionary prism was hampered by poor recovery but showed that the accreted sediments consist mostly of indurated, highly fractured mudstone, siltstone, and

sandstone, with rare carbonate-cemented nodules. Low contents of calcium carbonate in the mudstone indicate deposition close to or below CCD. The accretionary-prism strata are upper Miocene to lower Pliocene, ranging in time from 5.0 Myr to 5.9 Myr on the basis of nanofossils events. The original depositional environment (i.e., prior to accretion) is difficult to pinpoint but probably consisted of a relatively fine-grained part of the paleo-trench wedge (Expedition 315 Scientists, 2009b).

The upper surface of the accretionary prism near Site C0002 displays a convoluted geometry on seismic profiles, above which sits a relatively transparent interval measuring ~50–100 m in thickness (Fig. 15.8). Locally, the transparent interval dips seaward, and in other places it fills topographic lows in the underlying prism. This geometry is consistent with hemipelagic settling

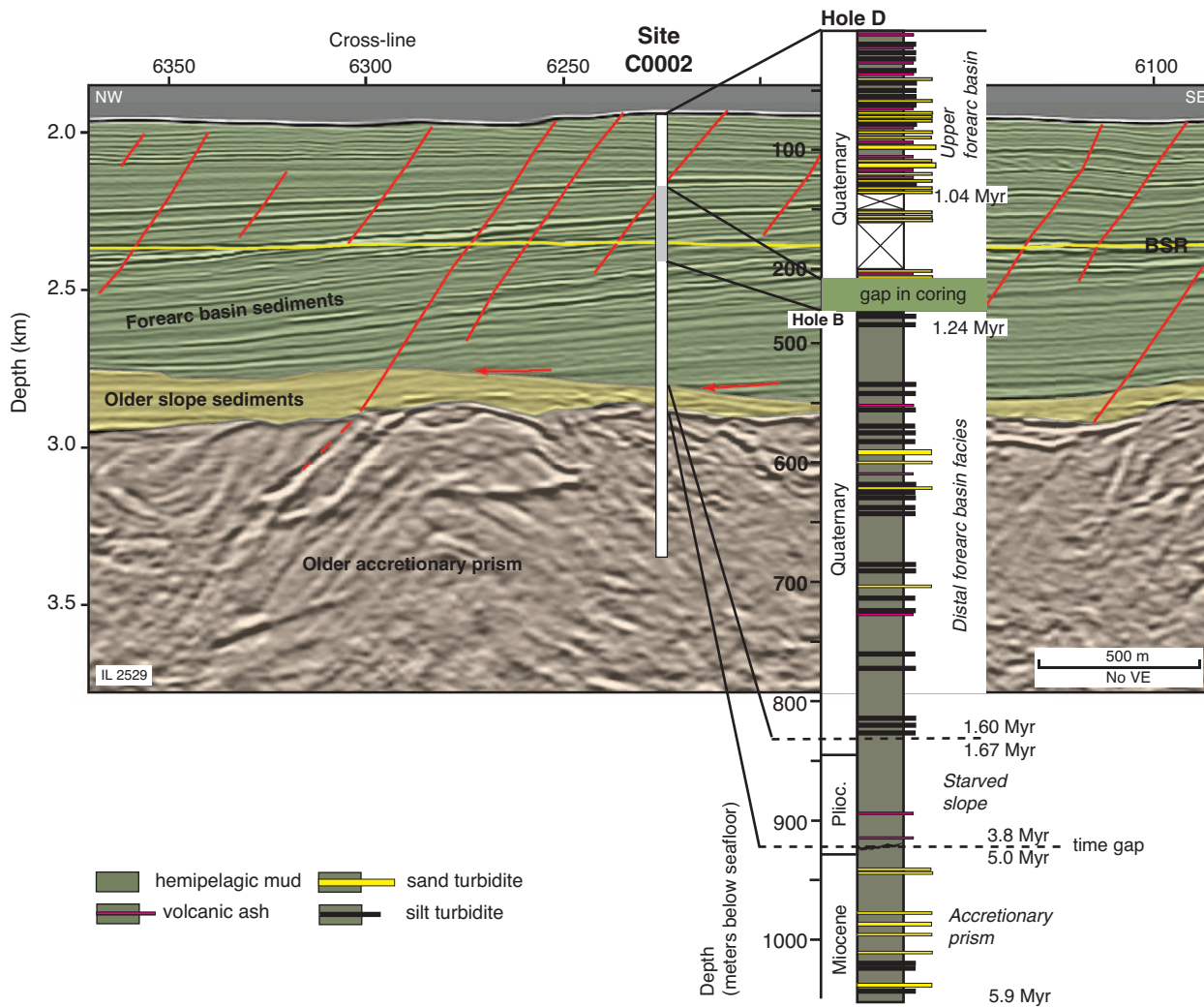


Fig. 15.8. Regional seismic line crossing IODP Site C0002, Kumano forearc basin. Seismic interpretation is from Moore et al. (2009). Also shown is the stratigraphic summary based on the results of coring and logging-while-drilling logging during Expeditions 314 and 315. Ages (Myr) are based on nannofossils zones.

onto an irregular substrate; the acoustic character is consistent with a monotonous lithology. Deposition probably occurred on the lower trench slope before that part of the prism was uplifted by slip along the megasplay fault (Moore et al., 2009). Coring confirmed that the transparent interval is composed of a condensed section of clay-rich hemipelagic mudstone. The mudstone is separated from the underlying prism by an angular unconformity, with a corresponding hiatus spanning from ~ 3.8 Myr above to ~ 5.0 Myr below. Strata above the boundary are within the lower Pleistocene to middle Pleistocene (3.79 Myr to 1.67 Myr on the basis of nannofossils events), and rates of sedimentation within that time interval were only

18–30 m/Myr. The condensed section accumulated at rates considerably slower than the typical rates for the Pleistocene slope apron. The content of calcite averages ~ 16 wt-% in the mudstone, which indicates deposition above CCD. Other noteworthy characteristics of this stratigraphic interval include sigmoidal, clay-filled vein structures (similar to those described by Ogawa and Miyata, 1985; Pickering et al., 1990; Brothers et al., 1996), a widespread ichnofauna of *Chondrites* and *Zoophycos*, local concentrations of glauconite, and sharp, irregular surfaces thought to represent firmgrounds (Expedition 315 Scientists, 2009b).

The acoustic character of most strata filling the Kumano Basin consists of landward-tilted,

high-amplitude, laterally continuous reflections, interpreted as a sequence of turbidites (Moore et al., 2009). The turbidites lap onto the older, condensed-mudstone unit (Fig. 15.8), but there is no evidence from coring to suggest an unconformable contact. The turbidites are tilted landward, presumably because slip along the megasplay fault promoted uplift at the seaward flank of the basin (Park et al., 2002). Continuation of the uplift also migrated the locus of sedimentation landward. The basin-fill strata are displaced by very young normal faults, many of which cut and displace the surface sediments. Coring demonstrated that the onset of turbidite sedimentation was abrupt, beginning at ~ 1.67 to 1.60 Myr. Thereafter, rates of sediment accumulation accelerated, reaching values of 400 to 800 m/My. These results show that the forearc basin is a relatively young feature with turbidite sedimentation not kicking into high gear until the middle to late Pleistocene.

The sedimentologic character of the forearc-basin turbidites (e.g., meso-scale cycles and individual graded beds) was recorded in impressive detail by LWD data (Expedition 314 Scientists, 2009a), but recovery of the sand beds was generally poor using the rotary coring system. The best information comes from the uppermost 140 m of sediment, which was cored using a hydraulic coring system; that interval consists of hemipelagic mud and numerous thin (1 – 15 cm) interbeds of normally graded silt, sandy silt, and sand, together with local layers of volcanic ash (Fig. 15.8). The thickest recovered sand bed is ~ 1.8 m. These beds display sharp bases, faint plane-parallel laminae, normal size grading, and diffuse tops. Silt and sand grains are composed mostly of quartz, feldspar, sedimentary and metasedimentary rock fragments (shale, argillite, chert, and quartz-mica grains), and a rich diversity of heavy minerals. Calcite content within the silty mud is generally low (average of 2 wt-%); presumably, this is because the biogenic contribution of nannofossils was diluted by high rates of terrigenous influx. Initiation of sand accumulation in a distal basin-plain type environment probably depended on the creation of suitable accommodation space by accelerated uplift along the megasplay fault, and that did not happen until ~ 1.55 Myr (Strasser et al., 2009). At the same time, the frequency of transport by sandy and silty turbidity currents from the shoreline also depends on high rates of erosion in the hinterland and incision of an effective delivery system into the upper continental slope, as represented by the Holocene

network of through-going submarine canyons and slope gullies (Fig. 15.1). Those delivery systems did not begin to reach a state of high activity until approximately 1.6 Myr, or roughly 3.4 Myr after frontal accretion of the underlying prism and ~ 0.35 Myr after the initial slip events on the megasplay.

CONCLUSIONS

Integration of geophysical data from a 3D seismic survey with coring and logging data from three recent IODP drilling expeditions has provided a wealth of new information about the lithostratigraphic and structural evolution of the Nankai subduction zone. We regard the following as among the more significant discoveries extracted from the IODP shipboard data.

Most of the information gathered from coring through the frontal fault zone is consistent with structural interpretations of the seismic data and generic models of frontal accretion. The accretionary prism within the Kumano transect area consists largely of offscraped sand-rich and gravel-rich packets, with an overall pattern of upward thickening and upward coarsening. This facies character is similar to what has been cored along the Muroto and Ashizuri transects of Nankai Trough, although the Kumano transect show a higher preponderance of coarse-grained channel-levee complexes. This makes sense given the closer proximity to Suruga Trough and Tenryu Canyon. Tectonic transfer of upper Shikoku Basin facies by thrust faulting to shallow depths of the frontal prism is unusual, however. Even more unexpected is the truncation of strata from the top of the Shikoku Basin section. We suggest that the missing sections were removed before frontal accretion by submarine slides on the flank of a subducting seamount, prior to gradual burial of the seamount beneath the landward-thickening trench wedge.

Most of the information garnered from coring around the up-dip terminus of the megasplay fault system is consistent with structural interpretations of the seismic data. One of the unexpected outcomes is the occurrence of an unconformity separating the slope apron from the underlying accretionary prism. The age of this unconformity seems to be time-transgressive (seaward younging), and the duration of the hiatus ranges from ~ 0.46 Myr to ~ 1.73 Myr. We suggest that the unconformity was created by persistent and widespread slumps and submarine slides during initial

uplift and oversteepening of the accretionary prism. The recovery of mass-transport complexes (mud-clast breccia and gravel) at two coring sites reinforces this interpretation. The shallow hanging-wall block to the megasplay fault is also unusual, consisting mostly of carbonate-poor hemipelagic mudstone. That fine-grained and monotonous lithology stands in sharp contrast to the sand-rich and gravel-rich accreted trench-wedge sediments in the frontal thrust zone.

Seismic reflection data clearly reveal the geometric patterns of infilling of the Kumano Basin, but coring demonstrates that nearly all of the basin-fill accumulated within the last 1.6 Myr. The basin rests above upper Miocene to lower Pliocene aged accretionary prism (5.0 Myr to 5.9 Myr). Turbidite deposition within the forearc basin was preceded by a long period of slow hemipelagic sedimentation; deposition of this condensed section extended from ~3.79 Myr to ~1.67 Myr. An angular unconformity separates the starved basin facies from the underlying accretionary prism, and the hiatus there lasted approximately 1.2 Myr. Acceleration of sediment delivery to the forearc basin lagged behind creation of the accommodation space via uplift along the megasplay fault, which began around 1.95 Myr. Rapid influx of turbidite sand to the forearc basin was probably enhanced by incision of a widespread system of submarine canyons and slope gullies across the upper continental margin, together with rapid uplift and erosion of sediment sources on the nascent Japanese Islands during the Pleistocene.

Collectively, these remarkable seismic-reflection records and coring results provide an outstanding view of the Nankai margin's evolution over the past 6 million years. New data from the NanTroSEIZE Kumano transect reinforce some basic contentions about how sedimentary systems behave in subduction zones. Subduction inputs change in intricate ways along the strike length of the subduction zone, particularly in response to basement topography, and those variations heavily influence how the accretionary prism evolves. We also see dynamic interplays working in the other direction, particularly with respect to offsets along the megasplay fault, remobilization of slope sediments by submarine slides, and creation of accommodation space for turbidite basins. This 3D complexity of structural and lithostratigraphic evolution certainly needs to be taken into account when interpreting ancient analogs in the rock record.

REFERENCES

- Aoki, Y., Tamano, T., and Kato, S. (1982) Detailed structure of the Nankai Trough from migrated seismic sections. In Watkins, J.S., and Drake, C.L., eds., *Studies in Continental Margin Geology*. Am. Assoc. Petrol. Geol. Memoir, 34, 309–322.
- Ashi, J., Lallemand, S., Masago, H., and the Expedition 315 Scientists (2009) Expedition 315 summary. In Kinoshita, M., Tobin, H., Ashi, J., Kimura, G., Lallemand, S., Screamton, E.J., Curewitz, D., Masago, H., Moe, K.T., and the Expedition 314/315/316 Scientists, Proc. IODP, 314/315/316: Washington DC, Integrated Ocean Drilling Program Management International, Inc. doi:10.2204/iodp.proc.314315316.121.2009.
- Bangs, N.L., Shipley, T.H., Gulick, S.P.S., Moore, G.F., Kuromoto, S., and Nakamura, Y. (2004) Evolution of the Nankai Trough décollement from the trench into the seismogenic zone: inferences from three-dimensional seismic reflection imaging. *Geology*, 32 (4), 273–276. doi: 10.1130/G20211.1.
- Bangs, N.L.B., Gulick, S.P.S.A., and Shipley, T.H. (2006) Seamount subduction erosion in the Nankai Trough and its potential impact on the seismogenic zone. *Geology*, 34 (8), 701–704. doi: 10.1130/G22451.1.
- Beaudry, D., and Moore, G.F. (1985) Seismic stratigraphy and Cenozoic evolution of west Sumatra forearc basin. *AAPG Bull.*, 69 (5), 742–759.
- Brothers, R.J., Kemp, A.E.S., and Maltman, A.J. (1996) Mechanical development of vein structures due to the passage of earthquake waves through poorly consolidated sediments. *Tectonophysics*, 260 (4), 227–244. doi: 10.1016/0040-1951(96)00088-1.
- Carlson, P.R., and Nelson, C.H. (1987) Marine geology and resource potential of Cascadia Basin. In *Geology and Resource Potential of the Continental Margin of Western North America and Adjacent Ocean Basins – Beaufort Sea to Baja California*, Scholl, D.W., Grantz, A., and Vedder, J., eds., Houston, TX, Circum-Pacific Council. *Energy Miner. Res.*, 523–536.
- Clift, P., and Vannucchi, P. (2004) Controls on tectonic accretion versus erosion in subduction zones: implications for the origin and recycling of the continental crust. *Rev. Geophys.*, 42:RG2001. doi: 10.1029/2003RG000127.
- Coulbourn, W.T. (1986), Sedimentologic summary, Nankai Trough Sites 582 and 583, and Japan Trench Site 584. In Kagami, H., Karig, D.E., and Coulbourn, eds., *Init. Rpts. DSDP*, 87:909-926. Washington, DC, U.S. Government Printing Office.
- Expedition 314 Scientists (2009a) Expedition 314 Site C0002. In Kinoshita, M., Tobin, H., Ashi, J., Kimura, G., Lallemand, S., Screamton, E.J., Curewitz, D., Masago, H., Moe, K.T., and the Expedition 314/315/316 Scientists, Proc. IODP, 314/315/316: Washington DC, Integrated Ocean Drilling Program Management International, Inc. doi:10.2204/iodp.proc.314315316.114.2009.
- Expedition 314 Scientists (2009b) Expedition 314 Site C0006. In Kinoshita, M., Tobin, H., Ashi, J., Kimura, G., Lallemand, S., Screamton, E.J., Curewitz, D., Masago, H., Moe, K.T., and the Expedition 314/315/316 Scientists, Proc. IODP, 314/315/316: Washington DC (Integrated Ocean Drilling Program Management International, Inc.) doi:10.2204/iodp.proc.314315316.118.2009.

- Expedition 315 Scientists (2009a) Expedition 315 Site C0001. In Kinoshita, M., Tobin, H., Ashi, J., Kimura, G., Lallemand, S., Screaton, E.J., Curewitz, D., Masago, H., Moe, K.T., and the Expedition 314/315/316 Scientists, Proc. IODP, 314/315/316. Washington, DC, Integrated Ocean Drilling Program Management International, Inc. doi:10.2204/iodp.proc.314315316.123.2009.
- Expedition 315 Scientists (2009b) Expedition 315 Site C0002. In Kinoshita, M., Tobin, H., Ashi, J., Kimura, G., Lallemand, S., Screaton, E.J., Curewitz, D., Masago, H., Moe, K.T., and the Expedition 314/315/316 Scientists, Proc. IODP, 314/315/316: Washington DC (Integrated Ocean Drilling Program Management International, Inc.) doi:10.2204/iodp.proc.314315316.124.2009.
- Expedition 316 Scientists (2009a) Expedition 316 Site C0004. In Kinoshita, M., Tobin, H., Ashi, J., Kimura, G., Lallemand, S., Screaton, E.J., Curewitz, D., Masago, H., Moe, K.T., and the Expedition 314/315/316 Scientists, Proc. IODP, 314/315/316: Washington, DC, Integrated Ocean Drilling Program Management International, Inc. doi:10.2204/iodp.proc.314315316.133.2009.
- Expedition 316 Scientists (2009b) Expedition 316 Site C0006. In Kinoshita, M., Tobin, H., Ashi, J., Kimura, G., Lallemand, S., Screaton, E.J., Curewitz, D., Masago, H., Moe, K.T., and the Expedition 314/315/316 Scientists, Proc. IODP, 314/315/316: Washington DC, Integrated Ocean Drilling Program Management International, Inc. doi:10.2204/iodp.proc.314315316.134.2009.
- Expedition 316 Scientists (2009c) Expedition 316 Site C0007. In Kinoshita, M., Tobin, H., Ashi, J., Kimura, G., Lallemand, S., Screaton, E.J., Curewitz, D., Masago, H., Moe, K.T., and the Expedition 314/315/316 Scientists, Proc. IODP, 314/315/316: Washington DC, Integrated Ocean Drilling Program Management International, Inc. doi:10.2204/iodp.proc.314315316.135.2009.
- Expedition 316 Scientists (2009d) Expedition 316 Site C0008. In Kinoshita, M., Tobin, H., Ashi, J., Kimura, G., Lallemand, S., Screaton, E.J., Curewitz, D., Masago, H., Moe, K.T., and the Expedition 314/315/316 Scientists, Proc. IODP, 314/315/316: Washington DC, Integrated Ocean Drilling Program Management International, Inc. doi:10.2204/iodp.proc.314315316.136.2009.
- Fisher, D., Mosher, D., Austin, J.A., Jr., Gulick, S.S.P., Masterlark, T., and Moran, K. (2007) Active deformation across the Sumatran forearc over the December 2004 Mw 9.2 rupture. *Geology*, 35 (2), 99–102. doi: 10.1130/G22993A.1.
- Gulick, S.P.S., Bangs, N.L.B., Shipley, T.H., Nakamura, Y., Moore, G., and Kuramoto, S. (2004) Three-dimensional architecture of the Nankai accretionary prism's imbricate thrust zone off Cape Muroto, Japan: prism reconstruction via an echelon thrust propagation. *J. Geophys. Res.*, 109 (B2), B02105. doi: 10.1029/2003JB002654.
- Gutscher, M.-A., Kukowski, N., Malavielle, J., and Lallemand, S. (1998) Episodic imbricate thrusting and underthrusting: Analog experiments and mechanical analysis applied to the Alaskan accretionary wedge. *J. Geophys. Res.*, 103 (B5), 10161–10176.
- Ike, T., Moore, G.F., Kuramoto, S., Park, J.-O., Kaneda, Y., and Taira, A. (2008a) Tectonics and sedimentation around Kashinosaki Knoll: a subducting basement high in the eastern Nankai Trough. *Isl. Arc*, 17 (3), 358–375. doi: 10.1111/j.1440-1738.2008.00625.x.
- Ike, T., Moore, G.F., Kuramoto, S., Park, J.-O., Kaneda, Y., and Taira, A. (2008b) Variations in sediment thickness and type along the northern Philippine Sea plate at the Nankai Trough. *Isl. Arc*, 17 (3), 342–357. doi: 10.1111/j.1440-1738.2008.00624.x.
- Kagami, H., Karig, D.E., Coulbourn, W., et al. (1986) Init. Repts. DSDP, 87. Washington, DC, U.S. Government Printing Office.
- Karig, D.E., Ingle, J.C., Jr., et al. (1975) Init. Repts. DSDP, 31. Washington, DC, U. S. Government Printing Office. doi: 10.2973/dsdp.proc.31.1975
- Karig, D.E., Suparka, S., Moore, G.F., and Hehanussa, P.E. (1978) Structure and Cenozoic evolution of the Sunda Arc in the central Sumatra region. In Watkins, J.S., Montadert, L., and Dickerson, P.W., eds., *Geological and Geophysical Investigations of Continental Margins*. Am. Assoc. Petrol. Geol. Memoir, 29, 223–237.
- Kawamura, K., Ogawa, Y., Anma, R., Yokoyama, S., Kawakami, S., Dilek, Y., Moore, G.F., Hirano, S., Yamaguchi, A., Sasaki, T., and YK05-08 Leg 2 and YK06-02 Shipboard Scientific Parties (2009) Structural architecture and active deformation of the Nankai accretionary prism, Japan: Submersible survey results from the Tenryu submarine canyon. *Geol. Soc. Am. Bull.*, 121, 1629–1646. doi: 10.1130/B26219.1.
- Kobayashi, K., Kasuga, S., and Okino, K. (1995) Shikoku Basin and its margins. In Taylor, B., (Ed.), *Back-arc basins*. New York, Plenum, 381–405.
- Kopp, H., Flueh, E.R., Klaeschen, D., Bialas, J., and Reichert, C. (2001) Crustal structure of the central Sunda margin at the onset of oblique subduction. *Geophys. J. Int.*, 147, 449–474.
- Kopp, H., and Kukowski, N. (2003) Backstop geometry and accretionary mechanics of the Sunda margin. *Tectonics*, 22, 1072. doi: 10.1029/2002TC001420.
- Kulm, L.D., and Fowler, G.A. (1974) Oregon continental margin structure and stratigraphy: A test of the imbricate thrust model. In Burk, C.A., and Drake, C.L., eds., *The geology of continental margins*. New York, Springer-Verlag, 261–283.
- Lewis, S.D., Ladd, J.W., and Bruns, T.R. (1988) Structural development of an accretionary prism by thrust and strike-slip faulting: Shumagin region, Aleutian Trench. *Geol. Soc. Am. Bull.*, 100, 767–782.
- MacKay, M.E., Moore, G.F., Cochran, G.R., Moore, J.C., and Kulm, L.D. (1992) Landward vergence and oblique structural trends in the Oregon margin accretionary prism: Implications and effect on fluid flow. *Earth Planet. Sci. Lett.*, 109, 477–491.
- Marsaglia, K.M., Ingersoll, R.V., and Packer, B.M. (1992) Tectonic evolution of the Japanese Islands as reflected in modal compositions of Cenozoic forearc and backarc sand and sandstone. *Tectonics*, 11, 1028–1044.
- McCarthy, J., and Scholl, D.W. (1985) Mechanisms of subduction accretion along the central Aleutian Trench. *Geol. Soc. Am. Bull.*, 96, 691–701.
- Mikada, H., Moore, G.F., Taita, A., Becker, K., Moore, J.C., and Klaus, A., eds. (2005) Proc. ODP, Sci. Results, 190/196. www-odp.tamu.edu/publications/190196SR/190196sr.htm.
- Miyazaki, S., and Heki, K. (2001) Crustal velocity field of southwest Japan: subduction and arc-arc collision. *J. Geophys. Res.*, 106 (B3), 4305–4326. doi: 10.1029/2000JB900312.

- Moore, G.F., Curray, J.R., Moore, D.G., and Karig, D.E. (1980) Variations in geologic structure along the Sunda forearc, northeastern Indian Ocean. In Hayes, D.E., ed., The tectonic and geologic evolution of Southeast Asian seas and islands. *Am. Geophys. Union Geophysical Monograph*, 23, 145–160.
- Moore, G.F., Shipley, T.H., Stoffa, P.L., Karig, D.E., Taira, A., Kuramoto, S., Tokuyama, H., and Suyehiro, K. (1990) Structure of the Nankai Trough accretionary zone from multichannel seismic reflection data. *J. Geophys. Res.*, 95 (B6), 8753–8765. doi: 10.1029/JB095iB06p08753.
- Moore, G.F., Taira, A., Klaus, A., Becker, L., Boeckel, B., Cragg, B.A., Dean, A., Fergusson, C.L., Henry, P., Hirano, S., Hisamitsu, T., Hunze, S., Kastner, M., Maltman, A.J., Morgan, J.K., Murakami, Y., Saffer, D.M., Sánchez-Gómez, M., Screaton, E.J., Smith, D.C., Spivack, A.J., Steurer, J., Tobin, H.J., Ujiie, K., Underwood, M.B., and Wilson, M. (2001) New insights into deformation and fluid flow processes in the Nankai Trough accretionary prism: results of Ocean Drilling Program Leg 190. *Geochem., Geophys., Geosyst.*, 2 (10), 1058. doi: 10.1029/2001GC000166.
- Moore, G.F., Bangs, N.L., Taira, A., Kuramoto, S., Pangborn, E., and Tobin, H.J. (2007) Three-dimensional splay fault geometry and implications for tsunami generation. *Science*, 318 (5853), 1128–1131. doi: 10.1126/science.1147195.
- Moore, G.F., Park, J.O., Bangs, N.L., Gulick, S.P., Tobin, H.J., Nakamura, Y., Sato, S., Tsuji, T., Yoro, T., Tanaka, H., Uraki, S., Kido, Y., Sanada, Y., Kuramoto, S., and Taira, A. (2009) Structural and seismic stratigraphic framework of the NanTroSEIZE Stage 1 transect. In Kinoshita, M., Tobin, H., Ashi, J., Kimura, G., Lallemand, S., Screaton, E.J., Curewitz, D., Masago, H., Moe, K.T., and the Expedition 314/315/316 Scientists, eds., *Proc. IODP, 314/315/316*. Washington DC, Integrated Ocean Drilling Program Management International, Inc. doi:10.2204/iodp.proc.314315316.102.2009.
- Mountney, N.P., and Westbrook, G.K. (1996) Modeling sedimentation in ocean trenches: the Nankai Trough from 1 Myr to the present. *Basin Research*, 8, 85–101.
- Ogawa, Y., and Miyata, Y. (1985) Vein structure and its deformational history in the sedimentary rocks of the Middle America Trench slope off Guatemala, Deep Sea Drilling Project Leg 84. In von Huene, R., Aubouin, J., Ed., et al., *Init. Repts. DSDP, 84*, Washington, DC, U.S. Government Printing Office, 811–829. doi: 10.2973/dsdp.proc.84.136.1985.
- Okino, K., Shimakawa, Y., and Nagaoka, S. (1994) Evolution of the Shikoku Basin. *J. Geomagn. Geoelectr.*, 46, 463–479.
- Park, J.O., Tsuru, T., Kodaira, S., Cummins, P.R., and Kaneda, Y. (2002) Splay fault branching along the Nankai subduction zone. *Science*, 297 (5584), 1157–1160. doi: 10.1126/science.1074111.
- Pickering, K.T., Agar, S.M., and Prior, D.J. (1990) Vein structure and the role of pore fluids in early wet-sediment deformation, late Miocene volcanoclastic rocks, Miura Group, SE Japan. In Knipe, R.J., and Rutter, E.H., eds., *Deformation Mechanisms, Rheology and Tectonics*. *Geol. Soc. Spec. Publ.*, 54 (1), 417–430. doi: 10.1144/GSL.SP.1990.054.01.38.
- Pickering, K.T., Underwood, M.B., and Taira, A. (1993) Stratigraphic synthesis of the DSDP-ODP sites in the Shikoku Basin and Nankai Trough and accretionary prism. In Hill, I.A., Taira, A., Firth, J.V., et al. *Proc. ODP, Sci. Results*, 131, College Station, TX, Ocean Drilling Program, 313–330. doi:10.2973/odp.proc.sr.131.135.1993.
- Piper, D.J.W., von Huene, R., and Duncan, J.R. (1973) Late Quaternary sedimentation in the active eastern Aleutian Trench. *Geology*, 1 (1), 19–22.
- Scholl, D.W. (1974) Sedimentary sequences in the north Pacific trenches. In Burk, C.A., and Drake, C.L., eds., *The geology of continental margins*. New York, Springer-Verlag, 493–504.
- Screaton, E.J., Kimura, G., Curewitz, D., and the Expedition 316 Scientists (2009a) Expedition 316 summary. In Kinoshita, M., Tobin, H., Ashi, J., Kimura, G., Lallemand, S., Screaton, E.J., Curewitz, D., Masago, H., Moe, K.T., and the Expedition 314/315/316 Scientists, eds., *Proc. IODP, 314/315/316*. Washington, DC, Integrated Ocean Drilling Program Management International, Inc. doi:10.2204/iodp.proc.314315316.131.2009.
- Screaton, E.J., Kimura, G., Curowitz, D., and 25 others (2009b) Interactions between deformation and fluids in the frontal thrust region of the NanTroSEIZE transect offshore the Kii Peninsula, Japan: Results from IODP Expedition 316 Sites C0006 and C0007. *Geochem. Geophys. Geosyst.*, 10, Q0AD01. doi:10.1029/2009GC002713.
- Schweller, W.J., Kulm, L.D., and Prince, R.A. (1981) Tectonics, structure, and sedimentary framework of the Peru-Chile Trench. *Geol. Soc. Am. Memoir* 154, 323–349.
- Seno, T., Stein, S., and Gripp, A.E. (1993) A model for the motion of the Philippine Sea plate consistent with NUVEL-1 and geological data. *J. Geophys. Res.*, 98 (B10), 17941–17948. doi: 10.1029/93JB00782.
- Shimamura, K. (1989) Topography and sedimentary facies of the Nankai Deep Sea Channel. In Taira, A., and Masuda, F., eds., *Sedimentary facies in the active plate margin*. Tokyo, Terra Science, 529–556.
- Soh, W., and Tokuyama, H. (2002) Rejuvenation of submarine canyon associated with ridge subduction, Tenryu Canyon, off Tokai, central Japan. *Marine Geol.*, 187, 203–220.
- Steurer, J.F., and Underwood, M.B. (2003) Clay mineralogy of mudstones from the Nankai Trough reference sites and frontal accretionary prism. In Mikada, H., Moore, G.F., Taira, A., Becker, K., Moore, J.C., and Klaus, A., eds., *Proc. ODP, Sci. Results*, 190/196. College Station, TX, Ocean Drilling Program.
- Strasser, M., Moore, G.F., Kimura, G., Kitamura, Y., Kopf, A. J., Lallemand, S., Park, J.O., Screaton, E.J., Su, X., Underwood, M.B., and Zhao, X. (2009) Origin and evolution of a tsunamigenic splay fault. *Nature Geoscience*, 2 (9), 648–652. doi: 10.1038/ngeo609.
- Taira, A., and Ashi, J. (1993) Sedimentary facies evolution of the Nankai forearc and its implications for the growth of the Shimanto accretionary prism. In Hill, I.A., Taira, A., Firth, J.V., et al. eds., *Proc. ODP, Sci. Results*, 131, College Station, TX, Ocean Drilling Program, 331–341.
- Taira, A., Hill, I., Firth, J.V., et al. (1991) *Proc. ODP, Init. Repts.*, 131. College Station, TX, Ocean Drilling Program. doi: 10.2973/odp.proc.ir.131.1991.
- Thornburg, T.M., and Kulm, L.D. (1987) Sedimentation in the Chile Trench: depositional morphologies, lithofacies, and stratigraphy. *Geol. Soc. Am. Bull.*, 98, 33–52.

- Tobin, H.J., and Kinoshita, M. (2006) NanTroSEIZE: the IODP Nankai Trough Seismogenic Zone Experiment. *Sci. Drill.*, 2, 23–27. doi: 10.2204/iodp.sd.2.06.2006.
- Tobin, H., Kinoshita, M., Ashi, J., Lallemand, S., Kimura, G., Screaton, E., Moe, K.T., Masago, H., Curewitz, D., and the Expedition 314/315/316 Scientists (2009a) NanTroSEIZE Stage 1 expeditions: introduction and synthesis of key results. In Kinoshita, M., Tobin, H., Ashi, J., Kimura, G., Lallemand, S., Screaton, E.J., Curewitz, D., Masago, H., Moe, K.T., and the Expedition 314/315/316 Scientists, eds., *Proc. IODP, 314/315/316: Washington, DC, Integrated Ocean Drilling Program Management International, Inc.* doi:10.2204/iodp.proc.314315316.101.2009.
- Tobin, H., Kinoshita, M., Moe, K.T., and the Expedition 314 Scientists (2009b) Expedition 314 summary. In Kinoshita, M., Tobin, H., Ashi, J., Kimura, G., Lallemand, S., Screaton, E.J., Curewitz, D., Masago, H., Moe, K.T., and the Expedition 314/315/316 Scientists, eds., *Proc. IODP, 314/315/316: Washington, DC, Integrated Ocean Drilling Program Management International, Inc.* doi:10.2204/iodp.proc.314315316.111.2009.
- Underwood, M.B. (2007) Sediment inputs to subduction zones: why lithostratigraphy and clay mineralogy matter. In Dixon, T.H., and Moore, J.C., eds., *The seismogenic zone of subduction thrust faults*. New York, Columbia University Press, 42–85.
- Underwood, M.B., and Fergusson, C.L. (2005) Late Cenozoic evolution of the Nankai trench-slope system: evidence from sand petrography and clay mineralogy. In Hodgson, D.M., and Flint, S.S., eds., *Submarine slope systems: processes and products*. Special Publication, 244. *Geol. Soc. London*, 113–129.
- Underwood, M.B., and Moore, G.F. (1995) Trenches and trench-slope basins. In Busby, C.J., and Ingersoll, R.V., eds., *Tectonics of sedimentary basins*. Cambridge, MA, Blackwell Science, 179–220.
- Underwood, M.B., and Steurer, J. (2003) Composition and sources of clay from the trench slope and shallow accretionary prism of Nankai Trough. In Mikada, H., Moore, G.F., Taira, A., Becker, K., Moore, J.C., and Klaus, A., eds., *Proc. ODP, Sci. Results, 190/196* College Station, TX, Ocean Drilling Program.
- Underwood, M.B., Moore, G.F., Taira, A., Klaus, A., Wilson, M.E.J., Fergusson, C.L., Hirano, S., Steurer, J., and the Leg 190 Shipboard Scientific Party (2003) Sedimentary and tectonic evolution of a trench-slope basin in the Nankai subduction zone of southwest Japan. *J. Sediment. Res.*, 73 (4), 589–602.
- Underwood, M.B., Hoke, K.D., Fisher, A.T., Davis, E.E., Giambalvo, E., Zuhlsdorff, L., and Spinelli, G.A. (2005) Provenance, stratigraphic architecture, and hydrogeologic influence of turbidites on the mid-ocean ridge flank of northwestern Cascadia Basin, Pacific Ocean. *J. Sediment. Res.*, 75, 149–164.
- Underwood, M.B., Saito, S., Kubo, Y., and the Expedition 322 Scientists. (2010) Expedition 322 summary, in Saito, S., Underwood, M.B., Kubo, Y., and the Expedition 322 Scientists, eds., *Proc. IODP, 322*. Tokyo, Integrated Ocean Drilling Program Management International, Inc. doi:10.2204/iodp.proc.322.101.2010.
- Zang, S.X., Chen, Q.Y., Ning, J.Y., Shen, Z.K., and Liu, Y.G. (2002) Motion of the Philippine Sea plate consistent with the NUVEL-1A model. *Geophys. J. Int.*, 150 (3), 809–819. doi: 10.1046/j.1365-246X.2002.01744.x.